Talanta 119 (2014) 214–225

Contents lists available at ScienceDirect

Talanta

journal homepage: www.elsevier.com/locate/talanta

Electrochemical sensors using modified electrodes based on copper complexes formed with Algerian humic acid modified with ethylenediamine or triethylenetetramine for determination of nitrite in water

Chafia Ait Ramdane-Terbouche [a,b], Achour Terbouche [a,b], Safia Djebbar [b,*], Didier Hauchard [c,d]

[a] Scientific and Technical Research Center in Physical and Chemical Analysis, (CRAPC), Algiers 16004, Algeria
[b] Laboratory of Hydrometallurgy and Molecular Inorganic Chemistry, Faculty of Chemistry, University of Sciences and Technology Houari Boumediene (USTHB), Algiers 16111, Algeria
[c] Sciences Chimiques de Rennes, UMR CNRS 6226, Ecole Nationale Supérieure de Chimie de Rennes, Avenue du général Leclerc, CS 50837, 35708 Rennes Cedex 7, France
[d] Université Européenne de Bretagne, 12 Avenue Janvier, 35000 Rennes, France

ARTICLE INFO

Article history:
Received 1 May 2013
Received in revised form
20 October 2013
Accepted 22 October 2013
Available online 11 November 2013

Keywords:
Modified Algerian humic acid
Copper complexes
Electrochemical sensors
Detection of nitrite

ABSTRACT

The response and efficiency of new sensors for nitrite ions analysis have been studied electrochemically. These sensors were developed by modifying a carbon paste electrode (CPE) with copper (II) complexes formed with commercial (PFHA) and Algerian (YHA) humic acids and their modified compounds with ethylenediamine (EDA) or triethylenetetramine (TETA). The developed mechanism is based on the electrochemical oxidation of NO_2^- on the modified CPE for different nitrite concentrations. The obtained results showed that the carbon paste electrode modified with copper (II)–modified humic acids complexes (Cu–MHA) exhibited substantial electrocatalytic effect on the oxidation of nitrite anions compared with carbon paste electrode. The sensitivity of the modified CPE towards nitrite concentrations depends on the nature of the humic acid and its modified compounds. The measurements performed by using CPE/Cu–YHA-EDA and CPE/Cu–YHA-TETA gave the best sensitivity and a good linear response of current versus nitrite concentrations.

The oxidation peak current of nitrite at CPE/Cu–YHA-TETA and CPE/Cu–YHA-EDA electrodes in weak acid solution is proportional to the concentration of nitrite over the range 0–1.38×10^{-2} mol L^{-1} with a limit of detection (LOD) of 1.46 μmol L^{-1} (Sensitivity = 41.06 μA (mmol $L^{-1})^{-1}$ and 2.17 μmol L^{-1} (Sensitivity = 27.63 μA (mmol $L^{-1})^{-1}$, respectively. Compared to the sensors published in the literature, our CPE/Cu–YHA-TETA and CPE/Cu–YHA-EDA electrodes exhibit a good catalytic activity towards nitrite oxidation and a low limit of detection over a wide nitrite concentrations range.

1. Introduction

Humic acids have a large number of carboxylic acids, hydroxyl and phenolic groups. They have been used for the preparation of chemically modified electrodes [1–5]. According to the literature, the sensitivity and selectivity of the functional groups of humic substances towards some complexing agents is restricted [6]. Therefore, in order to get better complexation, it is important to modify the functional groups of humic acids.

In recent years, significant progress has been realized on the impact of pollution on the environment and human health. Water and food are the possible sources of contaminants such as nitrite ions (NO_2^-) which are the product of the oxidation of nitrogen by microorganisms in plants, soil or water.

The widespread presence of nitrite in food products and beverages [7–10] causes a reaction with amines and amides in the human stomach to form N-nitroso compounds. Some of these products are potent carcinogens in humans [11,12]. However, nitrites can cause removal of oxygen in the bloodstream after causing the catalytic oxidation of hemoglobin to methemoglobin [13,14]. Hence, the detection of these ions and the development of highly selective sensors have become important and inevitable.

To detect and determine the concentration of nitrite in water and food, various methods have been used such as spectrophotometry and spectrofluorimetry [15–22], chromatography [23–28], capillary electrophoresis chemiluminescence [29] and electrochemistry [30–37].

Because of their low cost, easy operation, high sensitivity and fast response, the electrochemical techniques have advantages for the determination of nitrite concentration in aqueous solutions.

---

* Corresponding author. Tel.: +213 21247959; fax: +213 2124731.
E-mail address: safia.djebbar@netcourrier.com (S. Djebbar).

0039-9140/$ - see front matter © 2013 Elsevier B.V. All rights reserved.
http://dx.doi.org/10.1016/j.talanta.2013.10.049

The detection of nitrite ions by using electro-oxidation of NO_2^- is more effective in deaerated solution because the presence of molecular oxygen may limit the determination of nitrite [38,39].

Using conventional solid electrodes such as platinum, gold and glassy carbon to study electrochemical behavior of nitrites showed their limits because several species may mask the surface of the electrode, inducing a decrease in its sensitivity and accuracy [39]. The studies of the electrochemical behavior of nitrite by using glassy carbon electrode indicated that the oxidation of nitrite involves a large overpotential at the surface of the electrode [40–43]. Indeed, the modified electrodes were developed to eliminate the phenomenon of a large overpotential.

In recent years, many modified electrodes with carbon composites were developed as electrochemical sensors to determine nitrite ions in solution such as hydrophobic ionic liquid/carbon nanotubes/chitosan [44], SWCNT-cobalt nanoparticles [45], multi-walled carbon nanotubes (MWNT)–poly(amidoamine) (PAMAM)–chitosan (CS) nanocomposite in the immobilization of Cytochrome c (Cyt c) [46], graphene nanosheets and carbon nanospheres mixture (GNS–CNS) [34], poly(3,4-ethylenedioxythiophene) (PEDOT)- and PEDOT/multi-wall carbon nanotubes-(PEDOT/MWCNTs) modified screen-printed carbon electrodes (SPCEs) [47], polythionine/carbon nanotube modified electrode [48], multi-walled carbon nanotubes, zinc oxide, and gold nanoparticles integrated composite electrode [49].

To our knowledge, there have been no previous publications citing the use of the electrodes based on the modified humic acid complexes to quantify nitrite ions in solution. In the present work, novel sensors (modified electrodes) based on copper (II)–humic acid (Cu–HA) and copper (II)–modified humic acid (Cu–MHA) complexes were developed to detect nitrite ions in solution.

The modified electrodes were prepared by mixing the carbon powder (GC) with copper complexes formed with different humic acids (Cu–YHA or Cu–PFHA) and their modified forms (Cu–YHA-EDA, Cu–YHA-TETA, Cu–PFHA-EDA or Cu–PFHA-TETA) obtained by chemical reaction with ethylenediamine (EDA) and triethylenetetramine (TETA). The response and efficiency of these sensors towards nitrite ions were investigated by using cyclic voltammetry, linear polarization resistance and chronocoulometry methods.

To evaluate the sensitivity and the limit of detection of the sensors in a wide concentration range of nitrite, a developed method is based on the electrocatalytic oxidation of nitrite at CPE/Cu–HA and CPE/Cu–MHA electrodes in acidic medium (pH=4.4)

2. Materials and methods

2.1. Apparatus and reagents

Electronic absorption measurements and fluorescence spectra were respectively recorded on a UV–visible Perkin-Elmer Lambda 35 spectrophotometer and VARIAN Model CARY Eclipse fluorescence spectrophotometer. CHNS analyses were recorded on a Perkin-Elmer Analyzer 2400.

Fourier transform infrared spectra were carried out using a FT-IR Perkin-Elmer Spectrum One spectrometer over the 4000–400 cm^{-1} range, spectrometry grade with a peak resolution of 4 cm^{-1} and 32 scan right. All ^1H NMR measurements were performed on a Bruker 400 MHz NMR spectrometer.

The microstructure, surface topography and chemical analysis of the surface of the modified electrodes were examined by a scanning electronic microscope coupled to EDS method (Hitachi TM-1000).

Electrochemical measurements were performed under a nitrogen atmosphere using potentiostat/galvanostat (EGG Princeton Applied Research Model 273 A) in which a working electrode was replaced with unmodified or modified paste electrode. Platinum wire and Ag/AgCl (3 M KCl) were used as counter and reference respectively.

pH measurements were performed with A Metrohm 827 pH Lab Meter. A Precia Labo analytical balance model BP 110S was used to weigh the products.

A Fisher Scientific Polystat 36 water bath equipped with a thermostat was used to maintain the temperature at 25 °C for all experiments.

A Gilson micropipette (capacity of 20 μL) was used to perform all titrations.

Before each experiment, all glassware were washed with EDTA buffer solution (pH=8) to prevent metal binding and contamination.

All reagents used in this work were of the highest purity and analytical grade from Merck or Fluka. The copper and nitrite solutions of different concentrations were prepared from stock solutions (0.1 mol L^{-1}) of pure nitrate copper and sodium nitrite salts in free CO_2 deionised water (resistivity ≥ 14 MΩ cm).

2.2. Preparation and characterization of samples

Six samples of HAs and their derivates were studied. PFHA was purchased as a sodium salt from Fluka (lot and filling code: 12041/1 20902) and purified. YHA was isolated from Algerian soil at the Yakouren forest (Algeria) and characterized [50]. The modified PFHA and YHA with ethylenediamine (EDA) and triethylenetetramine (TETA) (PFHA-EDA, YHA-EDA, PFHA-TETA and YHA-TETA) were prepared by following procedure:

The mixture of 1 g of each initial humic acid (PFHA or YHA) with 5 mL of thionyl chloride was stirred for 1 h and concentrated in a vacuum drier at room temperature for 24 h. Then, 5 mL of ethylenediamine or triethylenetetramine were added to the obtained solid. The mixture was stirred for 1 h and concentrated in a vacuum drier at room temperature for 48 h. The obtained solid was acidified with HCl (1 mol L^{-1}) to pH 2. The final product was filtered, washed with water, and then dried under vacuum at room temperature.

The reaction mechanism for the modification of humic acids is shown schematically in Scheme 1.

To synthesize Cu–HA and Cu–MHA complexes in the solid state, several experiments were performed according to the quantities of copper, and the measurements that provide complexes in solid form are as follows:

Copper–humic acid and copper–modified humic acid complexes were prepared through mixing 500 mg L^{-1} of HA or MHA with 20 mL of nitrate copper solution (0.1 mol L^{-1}). Then, the mixture was stirred for 24 h and concentrated in a vacuum drier at room temperature for 48 h.

The modified carbon pastes were prepared by mixing 10 mg of each humic acid or modified humic acid complexes with 300 mg graphite powder and paraffin oil. The humic acid complexes or derivatives, graphite powder and paraffin oil were well mixed to obtain a uniform paste.

The modified electrodes were prepared by packing the modified paste into a glass tube having a diameter of 3 mm. The electrode surface was polished before ash measurement.

For the characterization of each HA and MHA, the ratio of absorbances at 465 and 665 nm (E_{465}/E_{665} ratio) was obtained in $NaHCO_3$ (25 mL, 0.025 mol L^{-1}) [51].

Carboxyl group content and total acidity were calculated, respectively, by the calcium acetate and the barium hydroxide methods [52].

The calcium acetate method is based on the reaction of HA with an excess of 0.5 mol L^{-1} calcium acetate solution. Hydrogen ions of humic acid carboxyl groups are exchanged for calcium ions of calcium acetate. The acetic acid formed is titrated with 0.1 mol L^{-1} NaOH.

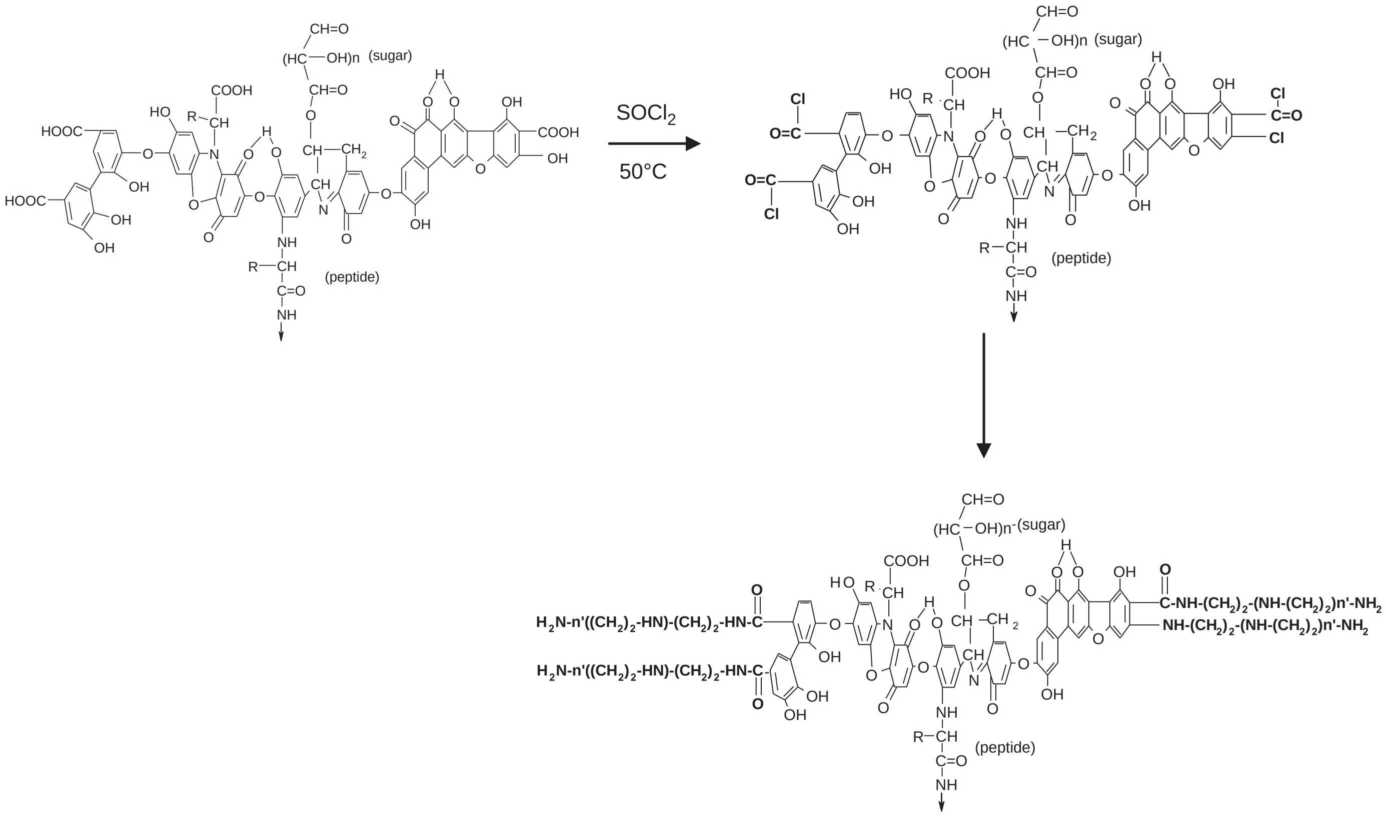

Scheme1. Proposed reaction scheme for the modification of the humic acids.

Phenolic hydroxyl group content is obtained as the difference between total acidity and carboxyl group content [53].

2.3. Electrochemical study and analysis of nitrite ions

The characterization of humic acids and modified humic acids at pH=7 was performed using three electrode cells. The working electrode was a glassy carbon electrode. A platinum wire and Ag/AgCl electrodes were used as auxiliary and reference electrodes, respectively.

The electrochemical oxidation behavior of nitrite in potassium chloride 0.1 mol L^{-1} was studied using carbon paste electrode modified with Cu–HA or Cu–MHA complexes, platinum wire and Ag/AgCl as working, auxiliary and reference electrodes, respectively.

To study the polarization resistance of all electrodes, the potential was scanned from the cathodic to anodic direction at a scan rate of 0.1 mV/s. The potential range of linear polarization experiments is ±25 mV.

Chronocoulometry measurements were obtained within 10 s with measuring period of 0.02 s.

To detect the nitrite ions by using CPE, CPE/Cu–HA and CPE/Cu–MHA electrodes, a suitable sensing potential in the limit current plateau region was determined between 0 and 1.5 V at a scan rate of 20 mV s^{-1} cyclic voltammetry method. The deaerated solution contains 0.1 mol L^{-1} KCl, 0.1 mol L^{-1} phosphate buffer solution (pH=4.4) and 1.38×10^{-2} mol L^{-1} of nitrite.

To determine the sensitivity and the limit of detection of CPE/Cu–HA and CPE/Cu–MHA sensors towards nitrite, the oxidation currents versus nitrite concentrations were recorded in 0–1.5 V potential range and the calibration curves were reported.

All nitrite, sodium phosphate and sodium chloride solutions were prepared with deionised water and the measurements were made in N_2 atmosphere at 25 °C.

3. Results and discussion

3.1. Chemical characterization of the compounds

3.1.1. Spectrometric, elemental analysis and acidic functional group contents.

The UV/vis spectra of PFHA and YHA humic acids (Fig. 1) showed broad spectra without the occurrence of specific bands and decreasing of absorbance as the wavelength increased. The spectra of the modified humic acids (PFHA-TETA and YHA-TETA) showed a strong band and a weak band with PFHA-EDA and YHA-EDA between 250 and 300 nm. These absorption bands are probably due to the primary amine groups (–CO–NH_2) indicating the formation of para-acylamino-groups (Ar-CONH–) which confirms the chemical modification of humic acids.

The high absorbance showed in the case of humic acids modified with TETA is due to its large number of amine groups comparing with humic acids modified with EDA.

Figs. S1 and S2 in Supplementary material show the fluorescence emission spectra of humic acids and modified humic acids. This technique is also used to distinguish between different humic substances [55,56]. The low intensity measured for MHA is due to the high molecular weight of humic compounds after modification with ethylenediamine and triethylenetetramine.

To confirm the modification of humic acids other analyzes were performed. Elemental analysis, acidic functional group and acidity contents of purified commercial humic acid, humic acid extracted from Yakouren forest soil and the modified humic acids are reported in the Table 1.

The modified humic acids (MHA) show higher N and C contents and a lower O content than unmodified humic acids (HA). These results indicate that a fair quantity of ethylenediamine and triethylenetetramine was bound to humic acids through carboxyl and phenolic groups.

The acidity group and oxygen contents in the modified humic acids are markedly lower than those of PFHA and YHA. Modified humic acids MHA have less total acidity than original HA. These results indicate that the modification is made through the carboxylic and phenolic groups.

Based on the literature [51], the highest E_{465}/E_{665} ratio of HA compared to MHA indicates that the modified humic acids have a higher molecular weight than the original humic acids.

3.1.2. Infrared spectra

Analysis of HA and MHA infrared spectra (Fig. 2) showed the following results:

The broad band located in the 3300–3400 cm^{-1} frequency region is due to the O–H stretching vibration of the phenolic, alcohol and carboxylic acid OH groups, and to the N–H stretching vibration of the amine groups (NH_2). The band observed between 1700 and 1750 cm^{-1} corresponds to C═O vibration of carboxylic and ketone or of carbonyl groups. A broad band in the 1265–1223 cm^{-1} frequency region produced by C–O of COOH of benzoic acids.

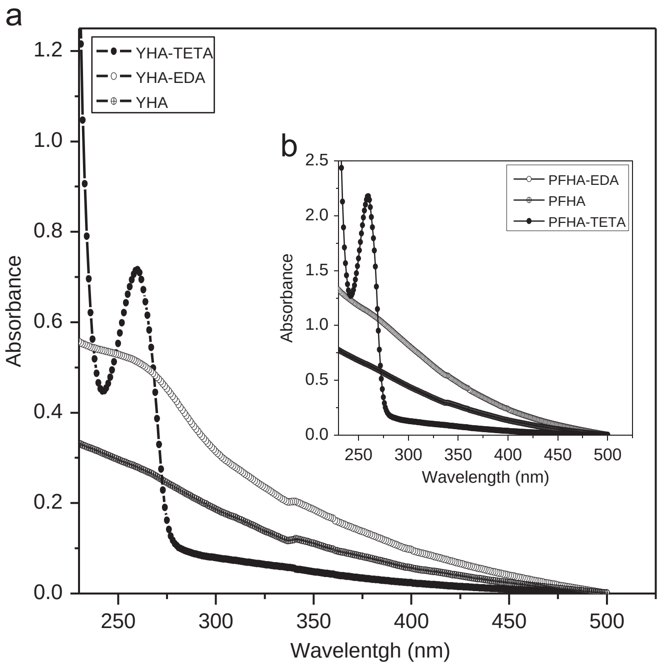

Fig. 1. Electronic spectra of (a) YHA and modified YHA and (b) PFHA and modified PFHA.

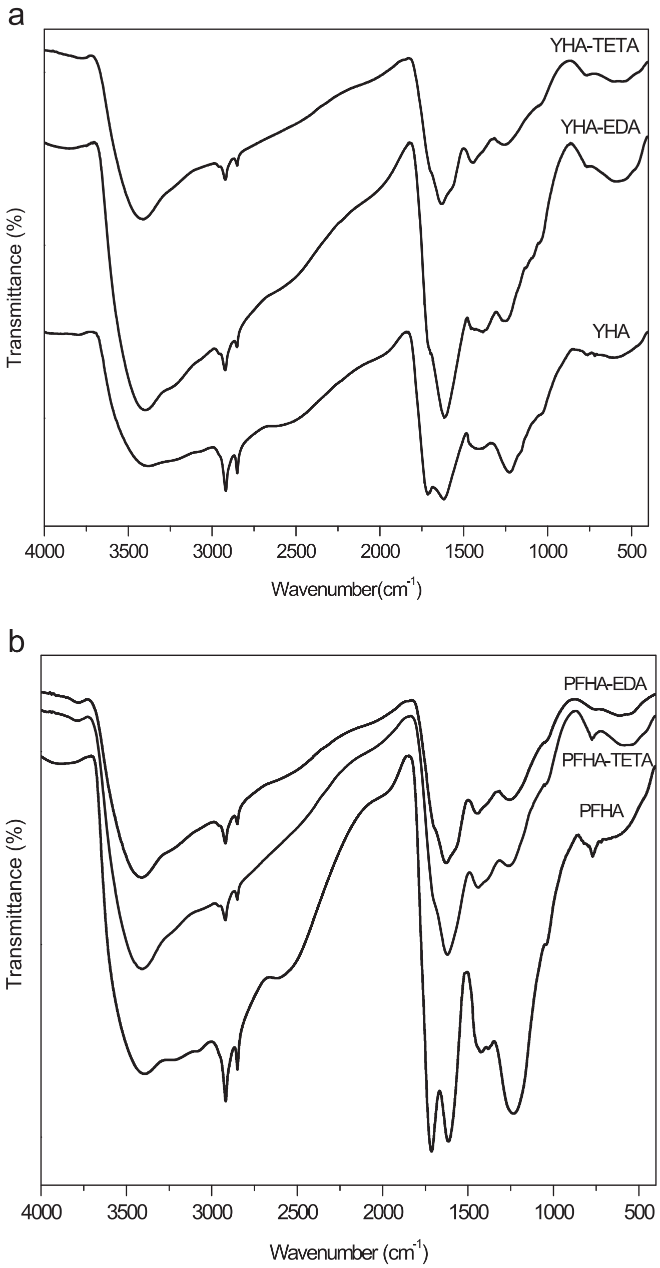

Fig. 2. FTIR spectra of (a) YHA and modified YHA and (b) PFHA and modified PFHA.

Table 1
Atomic ratios, E_{465}/E_{665}, acidic functional group and total acidity contents of humic acids and modified humic acids.

HAs	C%	H%	N%	O%	S%	E_{465}/E_{665}	COOH (mmol g^{-1})	Phenolic-OH (mmol g^{-1})	Total acidity (mmol g^{-1})
PFHA[50]	55.445 (0.035)	4.395 (0.085)	1.065 (0.005)	34.995	1.650	4.600 (0.002)	3.290 (0.008)	3.910 (0.005)	7.200 (0.003)
PFHA-EDA	57.500 (0.030)	4.780 (0.010)	2.300 (0.010)	33.810	1.610	4.470 (0.060)	2.780 (0.040)	2.810 (0.050)	5.590 (0.040)
PFHA-TETA	59.820 (0.020)	4.850 (0.020)	1.700 (0.010)	32.000	1.630	4.240 (0.030)	3.100 (0.010)	3.050 (0.030)	6.150 (0.080)
YHA[50]	54.615 (0.035)	4.970 (0.020)	3.405 (0.025)	35.560	0.250	4.665 (0.009)	3.425 (0.004)	4.325 (0.006)	7.750 (0.002)
YHA-EDA	59.200 (0.060)	6.550 (0.030)	5.900 (0.040)	28.110	0.240	4.390 (0.070)	0.290 (0.020)	2.110 (0.020)	2.400 (0.010)
YHA-TETA	60.250 (0.050)	5.700 (0.010)	4.10 (0.010)	29.740	0.210	3.810 (0.020)	0.040 (0.010)	4.030 (0.020)	4.070 (0.020)

Ash[50]: PFHA (2.45%); YHA(1.20%).

Compared with spectra of HA, the peak which represents C=O stretching of COOH (1700–1750 cm^{-1}) is shifted to 1696 cm^{-1}. The absorption of about 1265–1223 cm^{-1} disappeared in the spectra of MHA, indicating the disappearance of OH of carboxylic acid functional groups and the formation of para-acylamino-groups (Ar-CONH–, Ar represents aromatic ring) [54], respectively. The strong peaks near 1560 and 1568 cm^{-1} may be assigned to the vibration of N–H bond of EDA and TETA.

3.1.3. ^{1}H NMR spectra

^{1}H NMR spectra were obtained for basic structural information of HA and MHA (Fig. 3). The spectra showed a peak in the region of 8–8.5 ppm due to hydroxylic, carboxylic and amide protons, and the signals observed around 4.7 ppm are attributed to aromatic-OH groups (Ar-OH). The relative intensities of these peaks were decreased in the following order: HA > HA-EDA > HA-TETA indicating the elimination of a large amount of OH in hydroxylic and carboxylic groups of humic acids after their chemical modification.

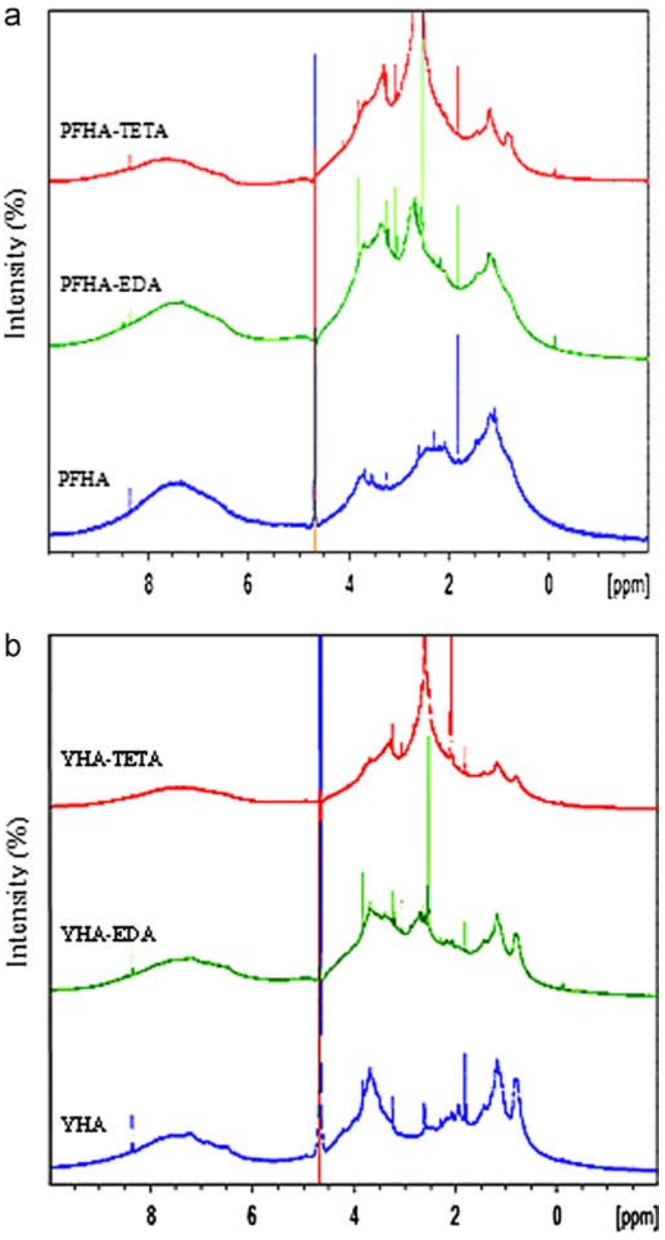

Fig. 3. ^{1}H NMR spectra of the humic acids and the modified humic acids in DMSO-d_6.

The wide signals observed in the 6–8 ppm resonance region can be assigned to aromatic protons.

In the spectra of MHA, the broad signals located in the range of 3.2–3.6 ppm were assigned to aliphatic amine (R-NH_2). The massifs observed between 2.7 and 3.0 ppm and intense peaks around 3.4 ppm were assigned to CH_2 protons in CH_2–NH_2 and CH_2–NH–COR groups, respectively. The intense peaks appeared at 3.1 ppm in the MHA spectra may be attributed to R-NH groups. These results confirm the modification of the humic acids.

The spectrum of YHA-TETA shows an intense peak at 2.2 ppm attributed to NH protons in the CH_2–NH–CH_2 groups, indicating that triethylenetetramine (TETA) coordinates more easily Yakouren humic acid than commercial humic acid which is more condensed than YHA [50].

The resonance at 1.8–2.1 ppm is attributed to the protons attached to aliphatic carbons of functional groups like carboxyl groups or aromatic rings. The massif in the region of 0.5–1.7 ppm is assigned to CH_2 and CH_3 attached to the aromatic ring.

3.1.4. Microstructure and surface topography

The surface topography of humic acids before and after modification with ethylenediamine (EDA) and triethylenetetramine (TETA) was observed by A scanning electronic microscope (SEM). The chemical modification of PFHA and YHA was observed by the change of the surface of humic acids after modification.

SEM photographs showed marked differences between HA, HA-EDA and HA-TETA samples in dispersion and the shape of the particles.

The interaction of ethylenediamine and triethylenetetramine with humic acid affects the surface of HA and caused the disappearance of a granular morphology of humic acids. HA presents more aggregates than HA-EDA and HA-TETA. The absence of aggregates on the surface of HA–TETA may be due to the existence of long aliphatic chains in theses macromolecules.

The morphologic results of PFHA, PFHA-EDA and PFHA-TETA (Fig. S3) are presented in Supplementary material.

EDS spectroscopy analysis of the compounds obtained upon complexation of Cu^{2+} with HA, HA-EDA and HA-TETA reveals that the formed materials contain copper, indicating the formation of Cu–HA and Cu–MHA complexes.

EDS spectra and photographs of Cu–YHA-TETA and Cu–PFHA-TETA complexes are given in Fig. 4, as an example.

Moreover, the presence of small white spots in SEM photographs is probably due to the strong complexation of copper with humic acids and modified humic acids. XRD analysis of the compounds exclude the hypothesis of Cu^{2+} deposition as salt form on the surface of HA and MHA.

3.1.5. Cyclic voltammetry

Cyclic voltammetry was used to study the electrochemical behavior of humic acids (PFHA and YHA) and their modified ones (PFHA-EDA, PFHA-TETA, YHA-EDA and YHA-TETA). The study was performed between -1.8 and 1.3 V using a potential scan rate of 20 mV s^{-1} and phosphate buffer pH 7.

Fig. 5 shows the cyclic voltammograms of humic acids and the modified humic acids with ethylenediamine and triethylenetetramine.

The voltammograms of MHA showed the disappearance of reduction peaks of OH groups observed at -1.46 V on voltammograms of unmodified humic acid, indicating the chemical modification of humic acids by EDA and TETA. This result confirms those obtained by the different characterizations reported above.

3.2. Stability study of the electrodes

The stability of the modified electrodes was studied by cyclic voltammetry in 0.1 mol L^{-1} KCl and phosphate buffer solution.

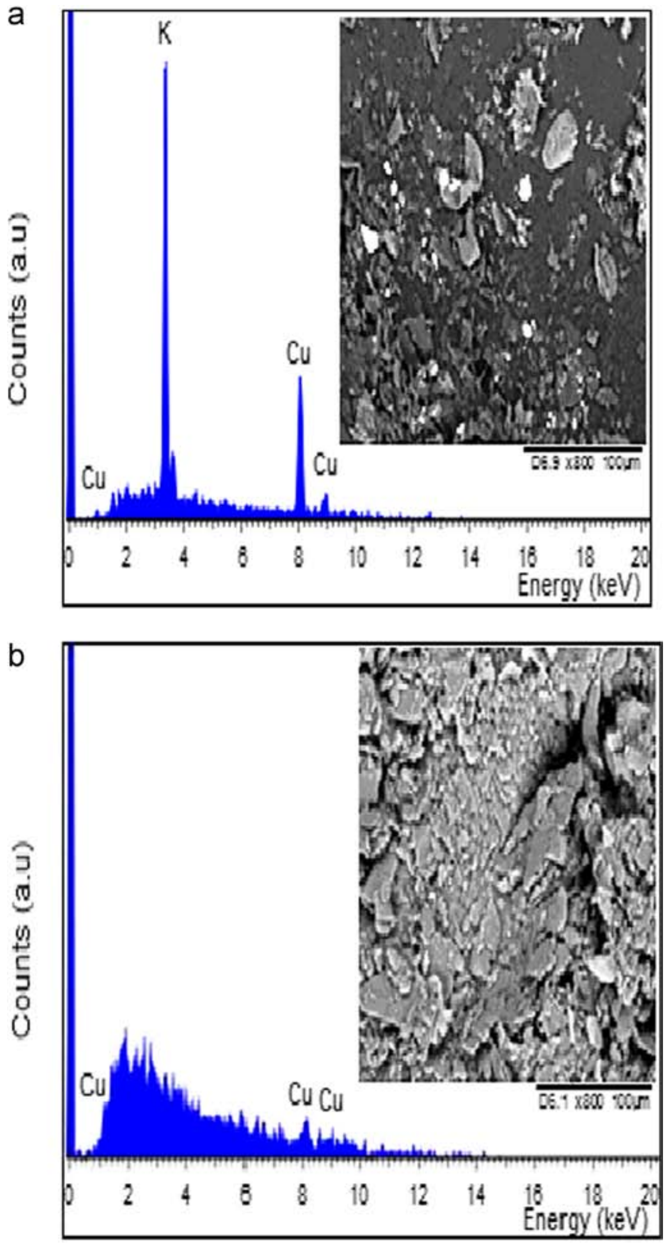

Fig. 4. SEM-EDS analysis of the copper complexes formed with modified humic acids. (a) Cu–YHA-TETA and (b) Cu–PFHA-TETA.

The twenty successive voltammograms obtained with the modified electrode CPE/Cu–YHA-EDA using a potential scan rate of 20 mV s^{-1} are reported in Fig. S4. The obtained results showed that the CPE/Cu–HA and CPE/Cu–MHA modified electrodes exhibit a well-defined cyclic voltammograms after scanning the potential between −0.8 and 1.3 V versus Ag/AgCl reference electrode for the first ten cycles. Therefore after ten successive cyclic voltammograms, a low increase in the intensity of the OH and copper reduction peaks was observed. It was also found that the currents decrease less than 3% when the electrode is stored in air at room temperature for two weeks.

3.3. Electrochemical behavior of the modified humic acid electrodes

The aim of this part of the work is to know the effect of the modification of humic acids on the electrochemical behavior of the nitrite ions.

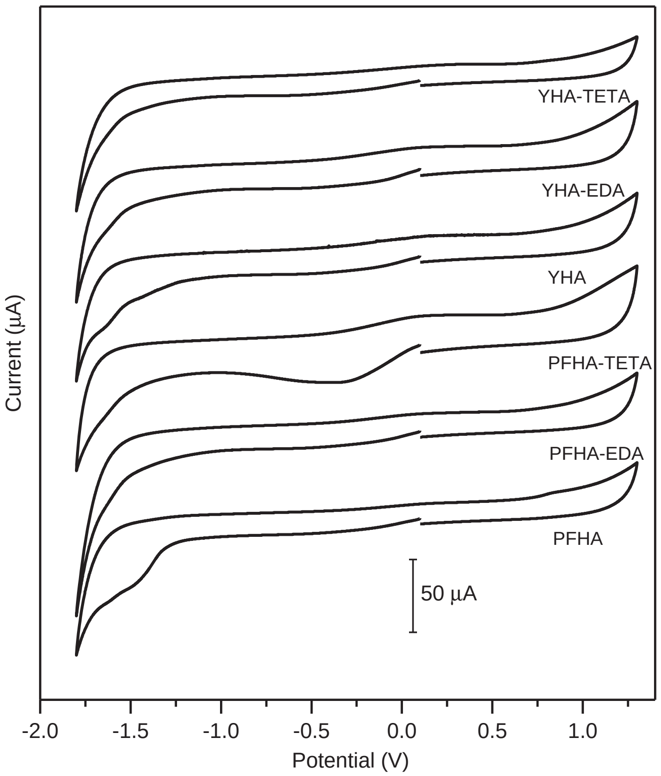

Fig. 5. Cyclic voltammograms of the humic acids and the modified humic acids at pH=7 (Na_2HPO_4/NaH_2PO_4: 0.01 mol L^{-1}) in $NaNO_3$ (0.1 mol L^{-1}).

In the absence of NO_2^-, the electrochemical behavior of the carbon paste electrode is different than the modified humic acid electrodes. The electrochemical study in 0.1 mol L^{-1} KCl at pH=4.4 using the carbon paste electrode showed that there was no current response in the potential range from 0 to −1.5 V. The cyclic voltammograms reported using the modified carbon paste with copper humic acid complexes (not shown here) showed reduction peaks between −0.7 and −0.2 V, corresponding to the electrochemical process of Cu(II)/Cu(I).

Varying the scan rate from 5 to 100 mV s^{-1}, the anodic and cathodic currents increase with scan rates, suggesting that the redox process is confined to the electrode surface.

The oxidation peak currents are linearly proportional to the square root of the scan rate ($\nu^{1/2}$), indicating that the electron transfer reaction is controlled by diffusion process.

3.4. Electro-oxidation behavior of nitrite on different electrodes

To investigate the electro-oxidation behavior of nitrite on different electrodes, the cyclic voltammograms have been recorded in the same experimental conditions as temperature, potential range and scan rate.

Cyclic voltammograms obtained using CPE, CPE/Cu–HA and CPE/Cu–MHA electrodes in 0.1 mol L^{-1} KCl and phosphate buffer solution containing 1.38×10^{-2} mol L^{-1} of nitrite are reported in Fig. 6. The voltammograms show an irreversible oxidation peak between 0.80 and 1.09 V, corresponding to the oxidation of NO_2^- to NO_3^- with the following process:

$$NO_2^- + H_2O \rightarrow NO_3^- + 2H^+ + 2e^-$$

The observed oxidation peak current of nitrite on the carbon paste electrode modified with Cu–HA and Cu–MHA is increased compared with the use of carbon paste electrode. The intensities oxidation peak current of nitrite on CPE/Cu–YHA-TETA and CPE/Cu–YHA-EDA are higher than those determined with the rest of

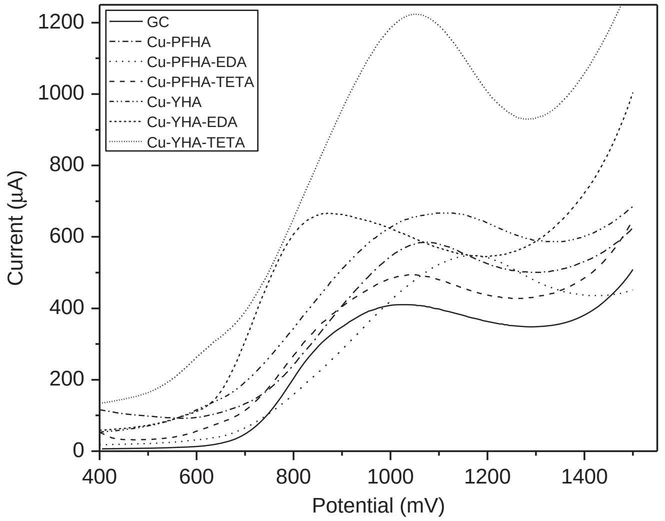

Fig. 6. Cyclic voltammograms obtained using CPE, CPE/Cu–HA and CPE/Cu–MHA electrodes in 0.1 mol L^{-1} KCl and phosphate buffer solution: experimental conditions: temperature=25 °C; $[NO_2^-]=1.38\times10^{-2}$ mol L^{-1}; scan rate=20 mV s^{-1}.

electrodes. At pH=4.4 (acidic solution), YHA-TETA and YHA-EDA were positively charged due to the protonation of their amine groups which attracted large quantities of nitrite ions involving high current intensity.

The analysis of Fig. 6 shows that the oxidation peak potential of NO_2^- on the CPE/Cu–YHA-EDA modified electrode shifted negatively to 0.854 V ($i=669.2$ µA) compared to 1.068 V ($i=409.2$ µA) obtained with carbon paste electrode. This result indicates an effective electro-oxidation of nitrite ions on the CPE/Cu–YHA-EDA electrode. This is probably due to the large surface area which leads to an increased heterogeneous electron transfer and to a high electron transfer capacity. Cu–YHA-EDA complex is considered as an electron mediator on the surface of CPE/Cu–YHA-EDA electrode.

3.5. Effect of varying scan rate on electro-oxidation of nitrite

The transport characteristics of the CPE/Cu–YHA-EDA electrode were studied by cyclic voltammetry method with different scan rates in 0.1 mol L^{-1} KCl and buffer phosphate solution (pH=4.4) containing 1.38×10^{-2} mol L^{-1} nitrite. The results showed that the oxidation peak current increases with increasing scan rates, as observed in Fig. 7a.

Fig. 7b showed a linear correlation between the oxidation current and the square root of scan rate in the range 5–100 mV s^{-1} with a linear regression equation of $i_{pa}=78.897\times\nu^{1/2}-5.523$ and a correlation coefficient of 0.992, indicating that the kinetic of the overall process is controlled by diffusion process.

Fig. 7c reveals a positive shift in peak potential position (E_{pa}) with the scan rate (log v), indicating that the electro-oxidation process of nitrite is irreversible. E_{pa} changed linearly versus log v in the 5–100 mV s^{-1} scan rate interval with a linear regression equation of $E_{pa}=134.833$ log $v+726.561$ and a correlation coefficient $R^2=0.993$. Referring to the Tafel equation defining a totally irreversible electrochemical process [57]:

$$E_p=\frac{b}{2}\log\ v+K\ \left(K=\text{constant}, b=\frac{2.303RT}{(1-\alpha)nF}\right)$$

The Tafel slope $\frac{1.151RT}{(1-\alpha)nF}=134.833$

Assuming that the reaction of oxidation of nitrite involves the transfer of two electrons ($n=2$), the electron transfer coefficient determined using Tafel slope was $\alpha=0.99$. Based on the work of Soderberg et al. [58], this exceptional value ($\alpha=0.99$) indicates a better electrocatalytic mechanism for oxidation of nitrite, and the electrode surface is fine and homogeneous.

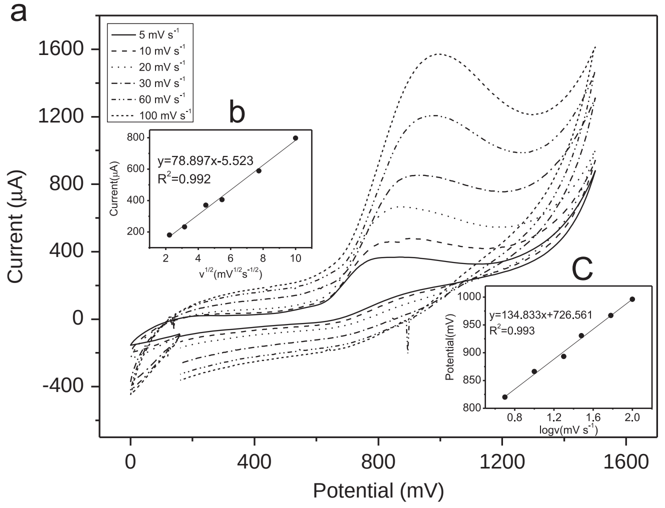

Fig. 7. (a) Cyclic voltammetry responses obtained at the carbon paste electrode modified with Cu–YHA-EDA in 0.1 mol L^{-1} KCl solution containing 1.38×10^{-2} mol L^{-1} NO_2^- versus scan rates; (b) current vs. square root of scan rate and (c) potential vs. log v. Experimental conditions: pH=4.4; temperature=25 °C.

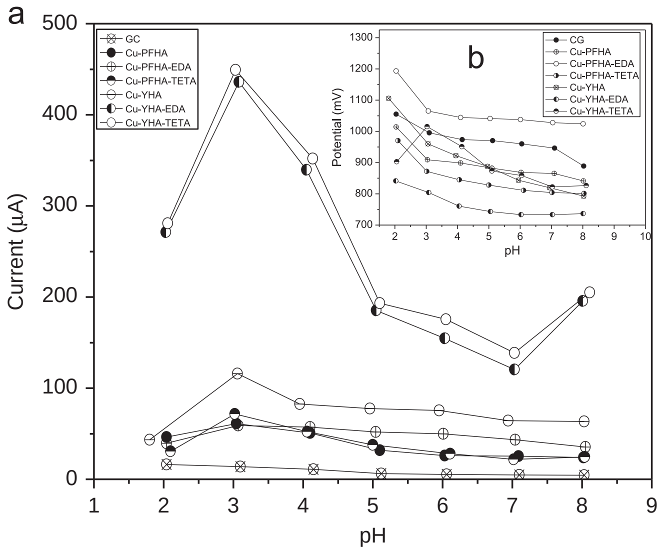

Fig. 8. (a) Oxidation current versus pH and (b) potential versus pH recorded with carbon paste electrode (CPE) and modified carbon paste electrode with copper complexes in 0.1 mol L^{-1} KCl. Experimental conditions: $[NO_2^-]=7.4\times10^{-4}$ mol L^{-1}; temperature=25 °C; scan rate=20 mV s^{-1}.

3.6. Effect of solution pH

The electrochemical behavior of nitrite (7.4×10^{-4} mol L^{-1}) on CPE, CPE/Cu–HA and CPE/Cu–MHA electrodes was studied at various pH values in 0.1 mol L^{-1} KCl.

The voltammograms of oxidation currents versus pH (Fig. 8a) showed that the current increases over a range of pH values from pH 2 to 3 and the maximum current is observed near pH=3.

The decreases of the oxidation current around pH=2 may be explained by the protonation of NO_2^- to obtain HNO_2 [59,60], or by its conversion to NO and NO_3^- [61,62] with the following reaction:

$$2H^+ + 3NO_2^- \rightarrow 2NO + NO_3^- + H_2O$$

For the pH values between 3 and 7, the current of oxidation decreases for most compounds. The results indicate that the Cu–HA and Cu–MHA complexes on carbon paste electrode are positively charged around pH=3 and attract the negatively charged ions (NO_2^-). The comparison of the electrochemical behavior of graphite carbon electrode and modified carbon paste electrodes shows that nitrite oxidation currents are more important in the case of modified electrodes. This indicates the main electrocatalytic role of copper complexes to promote the oxidation process of NO_2^-. Compared to the other complexes, Cu–YHA-TETA and Cu–YHA-EDA show the better electrocatalytic oxidation activity to nitrite. This may be due to the fact that YHA-TETA and YHA-EDA compounds are more aliphatic than the others. They have the widest distribution on graphite carbon. Therefore, there are high electrocatalytic active centers on CPE/Cu–YHA-TETA and CPE/Cu–YHA-EDA surfaces which involves a high electrocatalytic activity.

For the oxidation of nitrite ions, the curves representing the potential versus pH (Fig. 8b) showed that the potential shifts considerably for most electrodes to lower values from pH=1.95 to pH=4.4 and does not vary notably between pH=4.4 and 7. This reveals that the surface of electrodes has a better electrocatalytic activity for the oxidation of nitrite in this interval of pH. The sensitivity is enhanced working at pH=4.4 when the oxidation current is higher.

The maximum oxidation current was given at pH=3. pH Solution was chosen around 4 for all experiments because the potential of nitrite oxidation peak is low at this pH value.

Finally, the results of current and potential versus pH indicate that the electrode modified with Cu–YHA-EDA complex responds very effectively to the oxidation of nitrite compared to other electrodes.

3.7. Linear polarization resistance

The polarization resistance (R_p) is the reverse of the slope at the origin of the linear polarization curve in a very narrow voltage range around the zero current potential ($E_{i=}0$). R_p is related to the kinetics of the electrode reaction, which is more easily performed when the resistance is low.

The linear polarization resistance curves of CPE/Cu–HA and CPE/Cu–MHA systems in 0.1 mol L^{-1} KCl solution containing 1.38×10^{-2} mol L^{-1} NO_2^- are illustrated in Fig. 9.

The variation of current density versus potential is linear around zero current potential ($E_{i=}0$). The calculation of the linear polarization resistance showed that the systems formed with Yakouren humic acid (Cu–YHA-TETA: R_p=0.415 kΩ cm^2, Cu–YHA-EDA: R_p=1.14 kΩ cm^2 Cu–YHA: R_p=1.34 kΩ cm^2) are less resistant than those formed with purified commercial humic acid (Cu–PFHA-TETA: R_p=2.20 kΩ cm^2, Cu–PFHA-EDA: R_p=9.87 kΩ cm^2, Cu–PFHA: R_p=14.06 kΩ cm^2) and graphite carbon (GC: R_p=31.63 kΩ cm^2).

Cu–YHA-TETA and Cu–YHA-EDA systems have a low polarization resistance that causes a very important reaction rate on electrode. This proves the efficiency of CPE/Cu–YHA-TETA and CPE/Cu–YHA-EDA modified electrodes for the detection of nitrite ions.

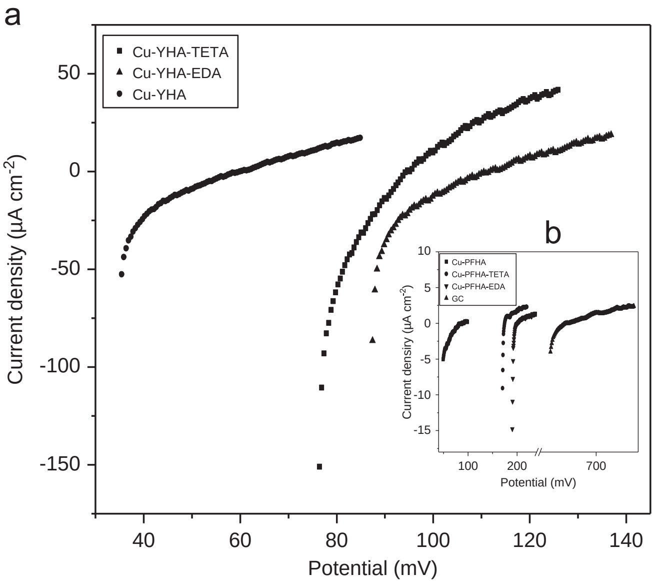

Fig. 9. Linear polarization curves of different systems (a) Cu–YHA-TETA, Cu–YHA-EDA and Cu–YHA (b) Cu–PFHA-TETA, Cu–PFHA-EDA, Cu–PFHA and GC in 0.1 mol L^{-1} KCl at pH=4.4 in the presence of 1.38×10^{-2} mol L^{-1} NO_2^-. Experimental conditions: temperature=25 °C; scan rate=0.1 mV s^{-1}.

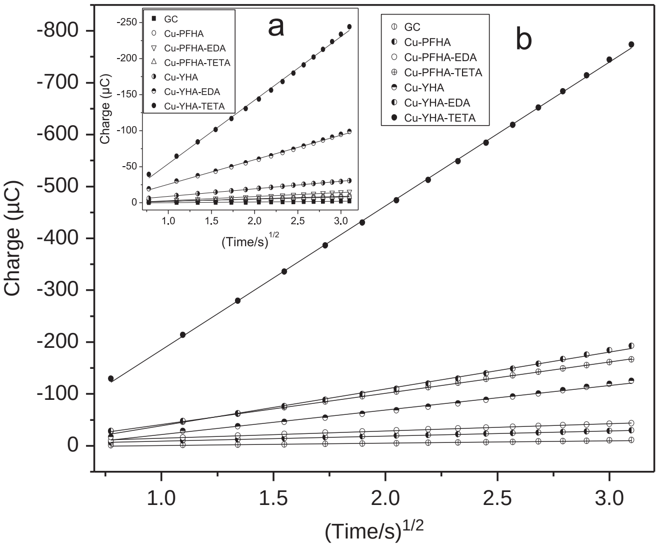

Fig. 10. Plots of Q vs. $t^{1/2}$ for different electrodes in 0.1 mol L^{-1} KCl at pH=4.4 in (a) absence and (b) presence of 1.38×10^{-2} mol L^{-1} NO_2^-. Experimental conditions: temperature=25 °C; measuring period=0.02 s.

3.8. Electrochemical reactivity

Chronocoulometry has been used to characterize the anodic process of 0.138 mmol L^{-1} nitrite at CPE, CPE/Cu–HA and CPE/Cu–MHA (Fig. S5 and Fig. 10). The plots of charge (Q) versus square root of time ($t^{1/2}$) (Fig. 10) show good linear relationships. According to the formula given by Anson [63], the relationship between the charge and square root of time can be described as follows:

$$Q(t) = \frac{2nFAcD^{1/2}t^{1/2}}{\pi^{1/2}} + Q_{dl} + Q_{ads}$$

where A is surface area of working electrode, c is concentration of substrate, D is diffusion coefficient, Q_{dl} is double layer charge which can be eliminated by background subtraction, Q_{ads} is Faradic charge. Other symbols have their conventional significance.

When $n=2$, $c=1.38 \times 10^{-2}$ mol L^{-1}, $A=0.071$ cm^2, from the slope and intercept of Q–$t^{1/2}$ line the diffusion coefficient (D) and faradic charge (Q_{ads}) can be calculated, respectively. Q_{ads} was obtained by the difference of two intercepts of the plot of Q vs. $t^{1/2}$ for curves in the absence and presence of nitrite.

Additionally, the surface coverage (Γ) can be determined according to the Faraday law:

$$Q_{ads} = nFA\Gamma$$

The linear relationship between Q and $t^{1/2}$ could be expressed as follows:

$Q = -277.616t^{1/2} + 92.708$ (CPE/Cu–YHA-TETA: $Q_{ads} = 58.589$ μC, $D = 1.69 \times 10^{-6}$ cm^2 s^{-1}, $\Gamma = 4.28 \times 10^{-8}$ mol cm^{-2}, $R^2 = 0.999$); $Q = -70.994t^{1/2} + 32.459$ (CPE/Cu–YHA-EDA: $Q_{ads} = 24.033$ μC, $D = 1.11 \times 10^{-7}$ cm^2 s^{-1}, $\Gamma = 1.76 \times 10^{-9}$ mol cm^{-2}, $R^2 = 0.996$); $Q = -47.224t^{1/2} + 25.520$ (CPE/Cu–YHA: $Q_{ads} = 23.938$ μC, $D = 4.89 \times 10^{-8}$ cm^2 s^{-1}, $\Gamma = 1.74 \times 10^{-9}$ mol cm^{-2}, $R^2 = 0.992$); $Q = -60.230t^{1/2} + 19.218$ (CPE/Cu–PFHA-TETA: $Q_{ads} = 18.398$ μC, $D = 7.96 \times 10^{-8}$ cm^2 s^{-1}, $\Gamma = 1.39 \times 10^{-9}$ mol cm^{-2}, $R^2 = 0.999$); $Q = -14.036t^{1/2} - 0.419$ (CPE/Cu–PFHA-EDA: $Q_{ads} = 3.177$ μC, $D = 4.34 \times 10^{-9}$ cm^2 s^{-1}, $\Gamma = 2.31 \times 10^{-10}$ mol cm^{-2}, $R^2 = 0.997$); $Q = -9.786t^{1/2} + 0.856$ (CPE/Cu–PFHA: $Q_{ads} = 0.298$ μC, $D = 2.10 \times 10^{-9}$ cm^2 s^{-1}, $\Gamma = 5.07 \times 10^{-11}$ mol cm^{-2}, $R^2 = 0.999$); and $Q = -4.574t^{1/2} + 4.0167$ (CPE: $Q_{ads} = 3.089$ μC, $D = 4.59 \times 10^{-10}$ cm^2 s^{-1}, $\Gamma = 2.25 \times 10^{-10}$ mol cm^{-2}, $R^2 = 0.971$).

These results showed that the values of the Faradic charge (Q_{ads}), surface coverage (Γ) and the diffusion coefficient (D) of nitrite ions are greater especially after modification of CPE by Cu–YHA-TETA and Cu–YHA-EDA, which would enhance the current response. This may be explained by the fact that, in the acidic solution, the Cu–YHA-TETA and Cu–YHA-EDA complexes have a positive charge caused by the protonation of the amine groups of YHA-TETA and YHA-EDA. Cu–YHA-TETA and Cu–YHA-EDA attract large amount of NO_2^- ions involving high Faradic charge and high surface coverage.

4. Detection of nitrite on different electrodes

Cyclic voltammetry measurements were carried out at room temperature between 0 and 1.5 V. The oxidation currents of nitrite ions were performed using potential scan rate of 20 mV s^{-1}.

The potential range varying between 0.7 and 1.1 V represents the area where a good response of oxidation of nitrite was recorded in terms of stability and sensitivity.

The voltammograms representing the oxidation current versus concentration of nitrite obtained using carbon paste electrode modified with Cu–YHA-EDA (CPE/Cu–YHA-EDA) and carbon paste electrode (CPE) in 0.1 mol L^{-1} KCl at pH = 4.4 is reported in Fig. 11a and b, respectively. The adding of NO_2^- to the electrolyte solution showed an increase in the anodic peak current.

In the presence of Cu(II) complexes, the nitrite ions were conversed to nitrate ions with a high current intensity compared to the case when the complex is absent.

The proposed catalytic mechanism is given by the following reactions:

$$\mathrm{Cu^{II}(HA\ or\ MHA)^{+} \leftrightarrow Cu^{III}(HA\ or\ MHA)^{2+} + e^{-}} \quad (1)$$

$$\mathrm{NO_2^- + Cu^{III}(HA\ or\ MHA)^{2+} \leftrightarrow Cu^{II}(HA\ or\ MHA)^{+} + NO_2} \quad (2)$$

NO_2 conversed to the nitrite and nitrate ions by the following reaction [64]:

$$\mathrm{2NO_2 + H_2O \leftrightarrow NO_2^- + NO_3^- + 2H^+} \quad (3)$$

Combining Eqs. (2) and (3), reaction (4) was obtained:

$$\mathrm{NO_2^- + 2Cu^{III}(HA\ or\ MHA)^{2+} + H_2O \leftrightarrow NO_3^- + 2H^+ + 2Cu^{II}(HA\ or\ MHA)^{+}} \quad (4)$$

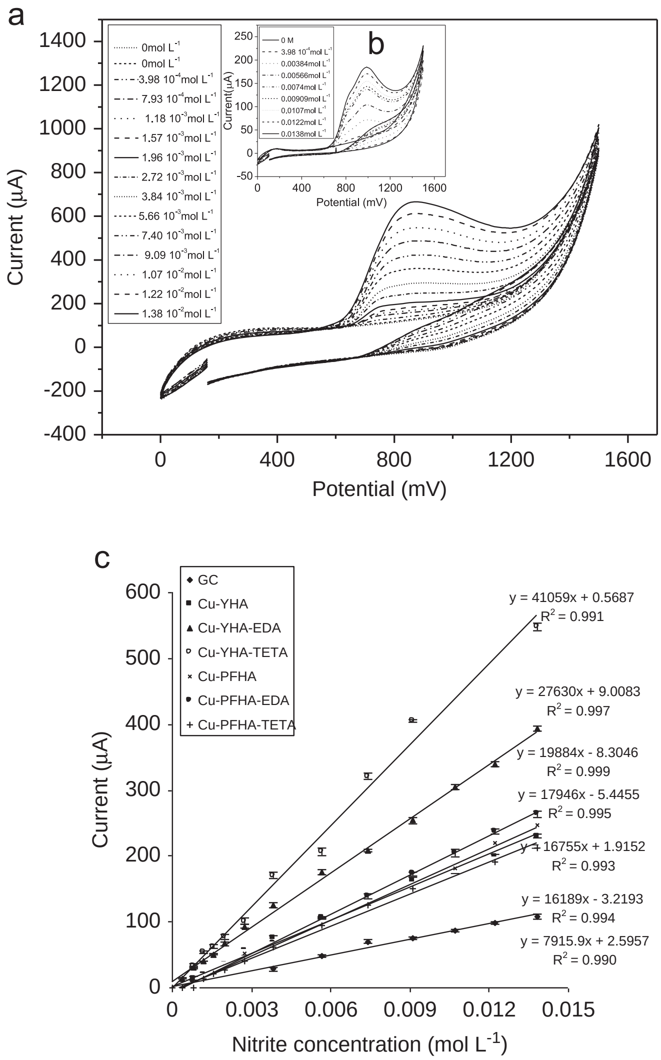

Fig. 11. Oxidation current versus concentration of nitrite ions obtained using (a) CPE/Cu–YHA-EDA modified electrode (b) CPE and (c) Linear relationship between the oxidation current and nitrite concentration obtained using CPE, CPE/Cu–HA and CPE/Cu–MHA in 0.1 mol L^{-1} KCl at pH = 4.4. Experimental conditions: temperature = 25 °C; scan rate = 20 mV s^{-1}.

Reporting i vs. [NO_2^-], a linear relationship was established between of the oxidation peak current and nitrite concentration in the range from 0 to 1.38×10^{-2} mol L^{-1} (Fig. 11c). The general equation was described below

$$i = a \times [NO_2^-] + b$$

The equations of the calibration curves determined using CPE, CPE/Cu–YHA, CPE/Cu–YHA-EDA, CPE/Cu–YHA-TETA, CPE/Cu–PFHA, CPE/Cu–PFHA-EDA and CPE/Cu–PFHA-TETA were

$i = 7915.9 \times [NO_2^-] + 2.5957 (R^2 = 0.990)$, $i = 16755.0 \times [NO_2^-] + 1.9152 (R^2 = 0.993)$, $i = 27630.0 \times [NO_2^-] + 9.0083 (R^2 = 0.997)$, $i = 41059.0 \times [NO_2^-] + 0.5687 (R^2 = 0.991)$, $i = 17946.0 \times [NO_2^-] - 5.4455 (R^2 = 0.995)$, $i = 19884.0 \times [NO_2^-] - 8.3046 (R^2 = 0.999)$ and $i = 16189.0 \times [NO_2^-] - 3.2193 (R^2 = 0.994)$, respectively.

According to Fig. 11c, the measurements performed using carbon paste electrodes modified with Cu–HA and Cu–MHA complexes gave highest sensitivity and good linearity ($R^2 = 0.990$) compared to those found using carbon paste electrode (CPE). The slopes of the calibration plots show that the response of CPE/Cu–HA and CPE/Cu–MHA electrodes towards nitrite ions is given in the following order:

$$\mathrm{YHA-TETA > YHA-EDA > PFHA-EDA > PFHA > YHA > PFHA-TETA > GC.}$$

Table 2
Comparison of CPE/Cu–HA and CPE/Cu–MHA electrodes with CPE electrode and author electrodes for the determination of nitrite.

Electrodes	Sensitivity μA (mmol L^{-1})$^{-1}$	Linear range (mmol L^{-1})	LOD (μmol L^{-1})	References
CPE	9.16	0–13.8	22.74	Present work
CPE/Cu–YHA	16.75	0–13.8	7.16	Present work
CPE/Cu–YHA-EDA	27.63	0–13.8	2.17	Present work
CPE/Cu–YHA-TETA	41.06	0–13.8	1.46	Present work
CPE/Cu–PFHA	17.95	0–13.8	8.36	Present work
CPE/Cu–PFHA-EDA	19.88	0–13.8	4.53	Present work
CPE/Cu–PFHA-TETA	16.19	0–13.8	5.56	Present work
Au/nanoparticles/poly(3-methylthiophene) composites electrode	–	0.010–1.00	2.3	[60]
Graphene and multiwall carbon nanotubes hybrid materials electrode	–	0.075–6.06	25.00	[65]
Cinder/PB-CPE	75.09	0 – 1.60	3.36	[66]
Polyaniline grafted nanodiamond	–	0.0005 –3.0	16	[67]
Nanocomposite and nanoporous polyaniline conducting polymers	–	0.0005 –1.4	24	[68]
PANI/gold electrode	110.4	0.01–9.0	5.0	[69]
Ferricyanide at the surface of carbon paste electrode	–	0.05–1.0	26.3	[70]

Under the optimum conditions for nitrite concentration range of 0 to 1.38×10^{-2} mol L^{-1} in the cyclic voltammetry, the limit of detection equals $3\ s/m$, where s is the standard deviation of the blank signal and m is the slope of the calibration plot. The determined sensitivity and limit of detection (LOD) of CPE electrode, modified electrodes and other published electrodes were compared and listed in Table 2.

According to the results found in this study, the modified electrodes with Cu–HA and Cu–MHA complexes showed a low limit of detection. CPE/Cu–YHA-TETA and CPE/Cu–YHA-EDA electrodes exhibited a detection limit of 1.46 µmol L^{-1} (Sensitivity = 41.06 μA (mmol L^{-1})$^{-1}$ and 2.17 µmol L^{-1} (Sensitivity = 27.63 μA (mmol L^{-1})$^{-1}$, respectively. These values are low compared to CPE (Sensitivity = 9.16 μA (mmol L^{-1})$^{-1}$, LOD = 22.74 µmol L^{-1}) and to those previously reported in the literature [60,64–69]. CPE/Cu–YHA-TETA and CPE/Cu–YHA-EDA electrodes exhibit good catalytic activity for the oxidation of nitrite with low LOD over a wide range of nitrite concentrations (mmol L^{-1} Scale). In the literature, most studies have not been carried out over a wide range of nitrite concentrations as in our work (0–1.38×10^{-2} mol L^{-1}). These results indicated that the proposed CPE/Cu–YHA-TETA and CPE/Cu–YHA-EDA electrodes are good sensors to detect of nitrite in a wide concentration range.

5. Conclusion

The aim of this study is to develop electrochemical sensors for detection of nitrite ions in aqueous solution. The preparation of the modified paste electrodes (sensors) was based on copper complexes formed with Algerian and commercial humic acids and their derivatives formed with EDA and TETA.

The characterization of the modified humic acids using different methods shows that the humic acids are associated to EDA and TETA through acidic and phenolic groups.

The electrochemical behavior of nitrite on different electrodes showed that the oxidation peak potential of NO_2^- on the CPE/Cu–YHA-EDA electrode shifted negatively compared to CPE and the rest of modified carbon paste electrodes. The determined electron transfer coefficient ($\alpha = 0.99$) indicates a better electrocatalytic mechanism for oxidation of nitrite ions on the CPE/Cu–YHA-EDA electrode.

The current and potential measurements versus pH reveal that nitrite ions are easily oxidized on the surface of CPE/Cu–YHA-TETA and CPE/Cu–YHA-EDA around pH = 4.4.

Linear polarization resistance showed that CPE/Cu–YHA-TETA and CPE/Cu–YHA-EDA electrodes are less resistant than CPE and the rest of the electrodes.

Chronocoulometry method revealed that the modified paste electrodes with Cu–YHA-TETA and Cu–YHA-EDA complexes respond very effectively to the oxidation of nitrite in acidic medium.

The plot of oxidation peak current versus nitrite concentration showed that the limit of detection of nitrite using CPE/Cu–YHA-TETA (1.46 µmol L^{-1}) and CPE/Cu–YHA-EDA (2.17 µmol L^{-1}) electrodes is low compared to LOD evaluated with CPE and other published electrodes.

The advantages of CPE/Cu–YHA-TETA and CPE/Cu–YHA-EDA electrodes are their stability, good electrocatalytic activity, low detection limit, low resistance and ability to make measurements in a wide range of nitrite concentrations, which is important for practical application on electrochemical sensors.

Acknowledgments

The authors appreciate Mr Jean-Paul GUEGAN and Isabelle MARLART of Ecole Nationale Supérieure de Chimie de Rennes UMR 6226: Institut des sciences chimiques de Rennes for the technical support of SEM-EDS and NMR spectroscopy.

Appendix A. Supplementary materials

Supplementary data associated with this article can be found in the online version at http://dx.doi.org/10.1016/j.talanta.2013.10.049.

References

[1] Z. Navrătilovă, P. Kula, Determination of mercury on a carbon paste electrode modified with humic acid, Electroanalysis 4 (1992) 683–687.
[2] Z. Navrătilovă, P. Kula, Modified carbon paste electrodes for the study of metal–humic substances complexation, Anal. Chim. Acta 273 (1993) 305–311.
[3] C.M. Wang, Q.Y. Sun, H.L. Li, Voltammetric behavior and determination of bismuth on sodium humate modified carbone-paste electrode, Electroanalysis 9 (1997) 645–649.
[4] A. Terbouche, C. Ait Ramdane-Terbouche, D. Hauchard, S. Djebbar, Evaluation of adsorption capacities of humic acids extracted from Algerian soil on polyaniline for application to remove pollutants such as Cd(II), Zn(II) and Ni (II) and characterization with cavity microelectrode, J. Environ. Sci. 23 (7) (2011) 1095–1103.
[5] A. Terbouche, C. Ait-Ramdane-Terbouche, S. Djebbar, O. Benali-Baitich, D. Hauchard, Effectiveness study of sensor based on modified cavity microelectrode by Algerian humic acid–polyaniline composites using square wave voltammetry, Sens. Actuators B 169 (2012) 297–304.
[6] J.E. Huheey, Inorganic Chemistry: Principles of Structure and Reactivity, third ed., Harper Collins, New York, 1983.
[7] I.E. Ezeagu, Occurrence of nitrate and nitrite in water and some alcoholic beverages in Nigeria, Nahrung 39 (1995) 530–534.

[8] M. Murata, M. Ishinaga, Nitrate and nitrite contents in vegetable juice, tea beverage and mineral water on the market, J. Food Hyg. Soc. Jpn. 46 (2005) 165–168.

[9] V.H.M. Luiz, L. Pezza, H.R. Pezza, Determination of nitrite in meat products and water using dapsone with combined spot test/diffuse reflectance on filter paper, Food Chem. 134 (2012) 2546–2551.

[10] E.A. Pereira, J.F.S. Petruci, A.A. Cardoso, Determination of nitrite and nitrate in Brazilian meats using high shear homogenization, Food Anal. Methods 5 (2012) 637–642.

[11] P. Fraser, Nitrates: Epidemiological Evidence, IARC ((Scientific Publication International Agency for Research on Cancer), Lyon, France. Publ. (1985) 183–194.

[12] S.S. Mirvish, Role of N-nitroso compounds (NOC) and N-nitrosation in etiology of gastric, esophageal, nasopharyngeal and bladder cancer and contribution to cancer of known exposures to NOC, Cancer Lett. 93 (1995) 17–48.

[13] A. Amine, G. Palleschi, Phosphate, nitrate, and sulfate biosensors, Anal. Lett. 37 (2004) 1–19.

[14] D. Zheng, C. Hu, Y. Peng, S. Hu, A carbon nanotube/polyvanillin composite film as an electrocatalyst for the electrochemical oxidation of nitrite and its application as a nitrite sensor, Electrochim. Acta 54 (2009) 4910–4915.

[15] V.V. Kuznetsov, S.V. Zemyatova, Flow-injection spectrophotometry of nitrites based on the diazotization reactions of azine dyes, J. Anal. Chem. 62 (2007) 637–644.

[16] H. Takiguchi, A. Tsubata, M. Miyata, T. Odake, H. Hotta, T. Umemura, K. Tsunoda, Liquid core waveguide spectrophotometry for the sensitive determination of nitrite in river water samples, Anal. Sci. 22 (2006) 1017–1019.

[17] T. Zhang, H. Fan, Q. Jin, Sensitive and selective detection of nitrite ion based on fluorescence superquenching of conjugated polyelectrolyte, Talanta 81 (2010) 95–99.

[18] V. Kumar, M. Banerjee, A. Chatterjee, A reaction based turn-on type fluorogenic and chromogenic probe for the detection of trace amount of nitrite in water, Talanta 99 (2012) 610–615.

[19] Z. Zhou, Q. Wang, Two emissive cellulose hydrogels for detection of nitrite using terbium luminescence, Sens. Actuators B 173 (2012) 833–838.

[20] L. Wang, B. Li, L. Zhang, L. Zhang, H. Zhao, Fabrication and characterization of a fluorescent sensor based on Rh 6G-functionlized silica nanoparticles for nitrite ion detection, Sens. Actuators B 171– (172) (2012) 946–953.

[21] H. Liu, G Yang, E.S. Abdel-Halim, J.J. Zhu, Highly selective and ultrasensitive detection of nitrite based on fluorescent gold nanoclusters, Talanta 104 (2013) 135–139.

[22] O. Zhang, Y. Wen, J. Xu, L. Lu, X. Duan, H. Yu, One-step synthesis of poly(3,4-ethylenedioxythiophene)–Au composites and their application for the detection of nitrite Synth, Metals 164 (2013) 47–51.

[23] S.B. Butt, M. Riaz, M.Z. Iqbal, Simultaneous determination of nitrite and nitrate by normal phase ion-pair liquid chromatography, Talanta 55 (2001) 789–797.

[24] R. Burakham, M. Oshima, K. Grudpan, S. Motomizu, Simple flow-injection system for the simultaneous determination of nitrite and nitrate in water samples, Talanta 64 (2004) 1259–1265.

[25] N. Bord, G. Crétier, J.L. Rocca, C. Bailly, J.P. Souchez, Simultaneous determination of inorganic anions and organic acids in amine solutions for sour gas treatment by capillary electrophoresis with indirect UV detection, J. Chromatogr. A 1100 (2005) 223–229.

[26] P. Niedzielski, I. Kurzyca, J. Siepak, A new tool for inorganic nitrogen speciation study: simultaneous determination of ammonium ion, nitrite and nitrate by ion chromatography with post-column ammonium derivatization by Nessler reagent and diode-array detection in rain water samples, Anal. Chim. Acta 577 (2006) 220–224.

[27] B. Prusisz, L. Jaskiewicz, P. Pohl, High-performance ion chromatography assessment of inorganic and organic nitrogen fractions in potatoes, Microchim. Acta 156 (2006) 219–223.

[28] S.M. Helmke, M.D. Duncan, Measurement of the NO metabolites, nitrite and nitrate, in human biological fluids by GC–MS, J. Chromatogr. B 851 (2007) 83–92.

[29] O. Nadzhafova, M. Etienne, A. Walcarius, Direct electrochemistry of hemoglobin and glucose oxidase in electrodeposited sol–gel silica thin films on glassy carbon, Electrochem. Commun. 9 (2007) 1189–1195.

[30] A.F. Lagalante, P.W. Greenbacker, Flow injection analysis of imidacloprid in natural waters and agricultural matrixes by photochemical dissociation, chemical reduction, and nitric oxide chemiluminescence detection, Anal. Chim. Acta 590 (2007) 151–158.

[31] B. Strehlitz, B. Grundig, W. Schumacher, P.M.H. Kroneck, K.D. Vorlop, H. Kotte, Nitrite sensor based on a novel highly sensitive nitrite reductase — mediator coupled amperometric detection, Anal. Chem. 68 (1996) 807–816.

[32] L.H. Larsen, L.R. Damgaard, T. Kjaer, T. Stenstrom, A.L. Jensen, N.P. Revsbech, Fast responding biosensor for on-line determination of nitrate/nitrite in activated sludge, Water Res. 34 (2000) 2463–2468.

[33] S.Q. Liu, H.X. Ju, Nitrite reduction and detection at a carbon paste electrode containing hemoglobin and colloidal gold, Analyst 128 (2003) 1420–1424.

[34] L. Cui, J. Zhu, X. Meng, H. Yin, X. Pan, S. Ai, Controlled chitosan coated Prussian blue nanoparticles with the mixture of graphene nanosheets and carbon nanoshperes as a redox mediator for the electrochemical oxidation of nitrite, Sens. Actuators B 161 (2012) 641–647.

[35] Q. Wang, Y. Yun, A nanomaterial composed of cobalt nanoparticles, poly(3,4-ethylenedioxythiophene) and graphene with high electrocatalytic activity for nitrite oxidation, Microchim. Acta 177 (2012) 411–418.

[36] C.Y. Lin, A. Balamurugan, Y.H. Lai, K.C. Ho, A novel poly(3,4-ethylenedioxythiophene)/iron phthalocyanine/multi-wall carbon nanotubes nanocomposite with high electrocatalytic activity for nitrite oxidation, Talanta 82 (2010) 1905–1911.

[37] Y. Li, Z. Ye, J. Zhou, J. Liu, G. Song, K. Zhang, B. Ye, A new voltammetric sensor based on poly(L-arginine)/graphene–nafion composite film modified electrode for sensitive determination of Terbutaline sulphate, J. Electroanal. Chem. 687 (2012) 51–57.

[38] C.A. Caro, F. Bedioui, J.H. Zagal, Electrocatalytic oxidation of nitrite on a vitreous carbon electrode modified with cobalt phthalocyanine, Electrochim. Acta 47 (2002) 1489–1494.

[39] M.H. Pournaghi-Azar, H. Dastangoo, Electrocatalytic oxidation of nitrite at an aluminum electrode modified by a chemically deposited palladium pentacyanonitrosylferrate film, J. Electroanal. Chem. 567 (2004) 211–218.

[40] W.E. Van Der Linden, J.W. Dieker, Glassy carbon as electrode material in electro-analytical chemistry, Anal. Chim. Acta 119 (1980) 1–24.

[41] J.E. Newbery, M.P. Lopez de Haddad, Amperometric determination of nitrite by oxidation at a glassy carbon electrode, Analyst 110 (1985) 81–82.

[42] H. Gunasingham, C.B. Tan, Platinum-dispersed Nafion film modified glassy… amperometric glucose enzyme electrode, Analyst 114 (1989) 695–698.

[43] E.H. Seymour, N.S. Lawrence, M. Pandurangappa, R.G. Compton, Indirect electrochemical detection of nitrite via diazotization of aromatic amines, Microchim. Acta 140 (2002) 211–217.

[44] F. Xiao, L. Liu, J. Li, J. Zeng, B. Zeng, Electrocatalytic oxidation and voltammetric determination of nitrite on hydrophobic ionic liquid–carbon nanotube gel–chitosan composite modified electrodes, Electroanalysis 20 (2008) 2047–2054.

[45] A.S. Adekunle, J. Pillay, K.I. Ozoemena, Probing the electrochemical behavior of SWCNT–cobalt nanoparticles and their electrocatalytic activities towards the detection of nitrite at acidic and physiological pH conditions, Electrochim. Acta 55 (2010) 4319–4327.

[46] Q. Chen, S. Ai, X. Zhu, H. Yin, Q. Ma, Y. Qiu, A nitrite biosensor based on the immobilization of cytochrome *c* on multi-walled carbon nanotubes–PAMAM–chitosan nanocomposite modified glass carbon electrode, Biosens. Bioelectron. 24 (2009) 2991–2996.

[47] C.Y. Lin, V.S. Vasantha, K.C. Ho, Detection of nitrite using poly(3,4-ethylenedioxythiophene) modified SPCEs, Sens. Actuators B 140 (2009) 51–57.

[48] C. Deng, J. Chen, Z. Nie, M. Yang, S. Si, Electrochemical detection of nitrite based on the polythionine/carbon nanotube modified electrode, Thin Solid Films 520 (2012) 7026–7029.

[49] A.J. Lin, Y. Wen, L.J. Zhang, B. Lu, Y. Li, Y.Z. Jiao, H.F. Yang, Layer-by-layer construction of multi-walled carbon nanotubes, zinc oxide, and gold nanoparticles integrated composite electrode for nitrite detection, Electrochim. Acta 56 (2011) 1030–1036.

[50] A. Terbouche, S. Djebbar, O. Benali-Baitich, D. Hauchard, Complexation study of humic acids extracted from Forest and sahara soils with zinc (II) and cadmium (II) by differential pulse anodic stripping voltammetry (DPASV) and conductimetric methods, Water Air Soil Pollut. 216 (2011) 679–691.

[51] Y. Chen, N. Senesi, M. Schnitzer, Information provided on humic substances by E4/E6 ratios, Soil Sci. Soc. Am. J. 41 (1977) 352–358.

[52] M. Schnitzer, S.U. Khan, Humic Substances in the Environment, Marcel Dekker, New York, 1972.

[53] M. Schnitzer, U.C. Gupta, Determination of acidity in soil organic matter, Soil Sci. Soc. Am. Proc. 29 (1965) 274–277.

[54] Y. Cheng, Organic Analysis (in chinese), Higher Education Press, Beijing, 1981.

[55] T.M. Miano, G. Sposito, J.P. Martin, Fluorescence spectroscopy of humic substances, Soil Sci. Soc. Am. J. 52 (1988) 1016–1019.

[56] N. Senesi, T.M. Miano, M.R. Provenzano, G. Brunetti, Spectroscopic and compositional comparative characterization of I.H.S.S. reference and standard fulvic and humic acids of various origin, Sci. Total Environ. 81/82 (1989) 143–146.

[57] A.J. Bard, L.R. Faulkner, Electrochemical Methods: Fundamentals and Applications, second ed., John Wiley and Sons, Hoboken, New Jersey, 2001.

[58] J.N. Soderberg, A.C. Co, A.H.C. Sirk, V.I. Birss, Impact of porous electrode properties on the electrochemical transfer coefficient, J. Phys. Chem. B 110 (2006) 10401–10410.

[59] A. Salimi, H. Mamkhezri, S. Mohebbi, Electroless deposition of vanadium–Schiff base complex onto carbon nanotubes modified glassy carbon electrode: application to the low potential detection of iodate, periodate, bromate and nitrite, Electrochem. Commun. 8 (2006) 688–696.

[60] X. Huang, Y. Li, Y. Chen, L. Wang, Electrochemical determination of nitrite and iodate by use of gold nanoparticles/poly(3-methylthiophene) composites coated glassy carbon electrode, Sens. Actuators B 134 (2008) 780–786.

[61] B. Kaita, A. Belhouari, L. Nadjo, R. Contant, Electrocatalysis by polyoxometalate/vbpolymer systems: reduction of nitrite and nitric oxide, J. Electroanal. Chem. 381 (1995) 243–250.

[62] M.A. Kamyabi, F. Aghajanloo, Electrocatalytic oxidation and determination of nitrite on carbon paste electrode modified with oxovanadium(IV)-4-methyl salophen, J. Electroanal. Chem. 614 (2008) 157–165.

[63] F. Anson, Application of potentiostatic current integration to the study of the adsorption of cobalt (III)-(ethylenedinitrilo (tetraacetate)) on mercury electrodes, Anal. Chem. 36 (1964) 932–934.

[64] R. Guidelli, F. Pergolo, G. Raspi, Voltammetric behavior of nitrite ion on platinum in neutral and weakly acidic media, Anal. Chem. 44 (1972) 745–755.

[65] F. Hu, S. Chen, C. Wang, R. Yuan, D. Yuan, C. Wang, Study on the application of reduced graphene oxide and multiwall carbon nanotubes hybrid materials for simultaneous determination of catechol, hydroquinone, p-cresol and nitrite, Anal. Chim. Acta 724 (2012) 40–46.

[66] J.M. Zen, A.S. Kumar, H.W. Chen, Electrochemical behavior of stable cinder/prussian blue analogue and its mediated nitrite oxidation, Electroanalysis 13 (2001) 1171–1178.

[67] M. Muchindu, T. Waryo, O. Arotiba, E. Kazimierska, A. Morrin, A.J. Killard, M.R. Smyth, N. Jahed, B. Kgarebe, P.G.L. Baker, E.I. Iwuoh, Electrochemical nitrite nanosensor developed with amine- and sulphate-functionalised polystyrene latex beads self-assembled on polyaniline, Electrochim. Acta 55 (2010) 4274–4280.

[68] A. Gopalan, K.P. Lee, S. Komathi, Bioelectrocatalytic determination of nitrite ions based on polyaniline grafted nanodiamond, Biosens. Bioelectron. 26 (2010) 1638–1643.

[69] M. Guo, J. Chen, J. Li, B. Tao, S. Yao, Fabrication of polyaniline/carbon nanotube composite modified electrode and its electrocatalytic property to the reduction of nitrite, Anal. Chim. Acta 532 (2005) 71–77.

[70] R. Ojani, J.B. Raoof, E. Zarei, Electrocatalytic reduction of nitrite using ferricyanide; application for its simple and selective determination, Electrochim. Acta 52 (2006) 753–759.